Journal of Groundwater Science and Engineering
ISSN 2305-7068
Indexed by ESCI CABI CSA Scopus GeoRef AJ CNKI

Application of the cumulative rainfall departure method in determination of deep groundwater recharge in Soc Trang Province, Vietnam

Tran Vu Long, Nguyen Bach Thao, Dao Duc Bang, Kieu Thi Van Anh, Vu Thu Hien, Duong Thi Thanh Thuy, Tran Quang Tuan, Nguyen Van Hoang, Doan Anh Tuan, Dang Tran Trung

Citation:
Long TV, Thao NB, Bang DD, *et al*. 2025. Application of the cumulative rainfall departure method in determination of deep groundwater recharge in Soc Trang Province, Vietnam. Journal of Groundwater Science and Engineering, 13(2): 180-192.

View online: https://doi.org/10.26599/JGSE.2025.9280048

Articles you may be interested in

Exploring the groundwater response to rainfall in a translational landslide using the master recession curve method and cross-correlation function
Journal of Groundwater Science and Engineering. 2024, 12(3): 237-252 https://doi.org/10.26599/JGSE.2024.9280018

Effects of urbanization on groundwater level in aquifers of Binh Duong Province, Vietnam
Journal of Groundwater Science and Engineering. 2021, 9(1): 20-36 https://doi.org/10.19637/j.cnki.2305-7068.2021.01.003

Groundwater recharge via precipitation in the Badain Jaran Desert, China
Journal of Groundwater Science and Engineering. 2024, 12(1): 109-118 https://doi.org/10.26599/JGSE.2024.9280009

Effects of climate anomaly on rainfall, groundwater depth, and soil moisture on peatlands in South Sumatra, Indonesia
Journal of Groundwater Science and Engineering. 2023, 11(1): 81-88 https://doi.org/10.26599/JGSE.2023.9280008

Impact of climate changes on Arizona State precipitation patterns using high-resolution climatic gridded datasets
Journal of Groundwater Science and Engineering. 2025, 13(1): 34-46 https://doi.org/10.26599/JGSE.2025.9280037

Quantifying groundwater recharge and discharge for the middle reach of Heihe River of China using isotope mass balance method
Journal of Groundwater Science and Engineering. 2021, 9(3): 225-232 https://doi.org/10.19637/j.cnki.2305-7068.2021.03.005

Journal of Groundwater Science and Engineering 13(2025) 180–192

Journal homepage: http://gwse.iheg.org.cn

Research Article

Application of the cumulative rainfall departure method in determination of deep groundwater recharge in Soc Trang Province, Vietnam

Tran Vu Long[1], Nguyen Bach Thao[1], Dao Duc Bang[1], Kieu Thi Van Anh[1], Vu Thu Hien[1], Duong Thi Thanh Thuy[1], Tran Quang Tuan[1], Nguyen Van Hoang[2*], Doan Anh Tuan[2], Dang Tran Trung[3]

[1] *Hanoi University of Mining and Geology, 18 Vien Street, Duc Thang Ward, Bac Tu Liem District, Hanoi, Vietnam.*
[2] *Institute of Geological Sciences, VAST, 84 Lane, Chua Lang Street, Lang Thuong Ward, Dong Da District, Hanoi, Vietnam.*
[3] *Center for Water Resources Warning and Forecast, Vietnam NAWAPI, No 93/95 Vu Xuan Thieu Street, Sai Dong Ward, Long Bien District, Hanoi, Vietnam.*

Abstract: Groundwater (GW) is a vital freshwater resource extensively exploited in the Vietnamese Mekong Delta, especially during the dry seasons. This study applies the Cumulative Rainfall Departure (CRD) method to estimate GW recharge in deep aquifers of Soc Trang Province, located in the southernmost region of Vietnam under a tropical climate. Monthly rainfall records and daily GW level data of the aquifers from 2010 to 2020 were used. The Pearson correlation between observed GW levels and CDR model GW levels exceeds 0.995, indicating high model accuracy. The analysis reveals that the CRD fractions for the Upper Pleistocene (qp_3), Middle Pleistocene ($qp_{2\text{-}3}$), Lower Pleistocene (qp_1), and Middle Pliocene (n_2^2) aquifers are 0.085%, 0.104%, 0.130%, and 0.180%, respectively, totaling approximately 0.5% of the annual rainfall. This corresponds to an annual GW recharge of 25.86 million m^3, or 70,850 m^3/day, equivalent to 70% of the current GW abstraction rate of 101,000 m^3/day. Given the critical role of GW as a freshwater source, implementing an enhanced GW recharge program using surface water and rainwater is strongly recommended. Additionally, the analysis suggests that the decline in GW levels due to abstraction corresponds to 0.85 times the mean annual precipitation, a finding that warrants further investigation.

Keywords: Mekong delta; Tropical climate; Groundwater (GW) level; Mean precipitation; Pearson correlation

Received: 19 Aug 2024/ Accepted: 25 Mar 2025/ Published: 10 May 2025

Introduction

Groundwater (GW) is a crucial water resource worldwide, particularly in arid and semi-arid regions (Parisa et al. 2023; Wang et al. 2024). In Asia, GW serves as a vital freshwater source but faces significant distribution disparities and unsustainable exploitation (Cheng et al. 2024). In the Mekong River Basin, where rapid population growth and increasing economic activities drive water demand, GW remains essential and readily available resource (Eunhee et al. 2017). Therefore, determination of the safe yield of GW is critical for sustainable management.

GW recharge is a key factor influencing the availability and sustainability of groundwater resources (Shamla and Marykutty, 2024). Estimating GW recharge is fundamental for effective water resource management in terms of quantity and quality. Recharge is particularly important for sustaining overexploited aquifers. For example, in the North China Plain, GW has been overdrawn since 2014, prompting the Ministry of Water Resources to implement GW recharge measures in

*Corresponding author: Nguyen Van Hoang, *E-mail address*: N_V_Hoang_VDC@yahoo.com

DOI: 10.26599/JGSE.2025.9280048

Long TV, Thao NB, Bang DD, et al. 2025. Application of the cumulative rainfall departure method in determination of deep groundwater recharge in Soc Trang Province, Vietnam. Journal of Groundwater Science and Engineering, 13(2): 180-192.

2305-7068/© 2025 Journal of Groundwater Science and Engineering Editorial Office This is an open access article under the CC BY-NC-ND license (http://creativecommons.org/licenses/by-nc-nd/4.0)

2018, achieving notable success (Meng et al. 2023).

GW recharge estimation is a complex and sensitive process, with significant variability in accuracy and uncertainty. Kinzelbach and Aeschbach (2002) categorized recharge estimation methods into four main types: 1) Direct measurements; 2) Water balance methods; 3) Darcyan methods; 4) Tracer methods. Their study discussed the advantages and limitations of each approach, particularly in terms of accuracy and uncertainty. More recently, Shamla and Marykutty (2024) provided a comprehensive analysis of GW recharge estimation techniques, highlighting their assumptions, benefits, limitations, and selection criteria.

The Cumulative Rainfall Departure (CRD) method, proposed by Bredenkamp et al. (1995), utilizes the relationship between groundwater level fluctuations and the deviations in rainfall from the mean of preceding periods. According to Kinzelbach and Aeschbach (2002), the method offers advantages such as simplicity and error stabilization due to long time series. However, its limitations include the need for a known storage coefficient, accurate discharge (including abstractions), and moderate accuracy. Despite these limitations, the CRD method has been widely applied by various researchers, including Djellali et al. (2023), Tesfaldet et al. (2020), Wang et al. (2024).

GW recharge occurs through various mechanisms, Xu and Beekman (2019) classify these into four main types: 1) Vertical water percolation through the unsaturated zone, reaching the water table; 2) Lateral and/or vertical inter-aquifer flow; 3) Artificial recharge, such as infiltration ponds or injection wells; and 4) Induced recharge from nearby surface water bodies (rivers, streams, lakes) as a result of GW abstraction.

The CRD method has been primarily applied to shallow aquifers. Xu and Van Tonder (2001) demonstrated its application in several shallow fractured aquifers with low storativity. Adams et al. (2003) employed the Chloride Mass Balance (CMB), Saturated Volume Fluctuation (SVF), and CRD methods to quantify GW recharge in the Central Namaqualand region of South Africa. Their findings indicated strong agreement between the SVF and CRD results, revealing higher recharge rates in mountainous areas compared to lower lying areas. Additionally, their study confirmed that GW recharge predominantly occurs through alluvial aquifers with significant soil cover.

Baalousha (2005) applied CRD method to quantify GW recharge in the Gaza Strip (Palestine), a transitional zone between the semi-humid region and the semi-arid loess plains. The aquifer in this region is primarily phreatic, with thickness varying from a few meters at the east to 170 m. It consists of Pleistocene calcareous sandstone and gravel, as well as Holocene sand interbedded with silt, clay, and conglomerate. The aquifer's storativity ranges from 0.0005 to 0.03. The study determined that average GW recharge ranges from 31.64% to 41.10%, with a mean value of 36.74%.

Rasoulzadeh and Moosavi (2007) utilized both the CRD and revised CRD methods to estimate GW recharge from rainfall in the Quaternary aquifer of the Tashk Lake area in Iran. The aquifer, with a thickness of 30 m to over 300 m, consists of rubble stone, gravel, sand, and silt with minor clay content. Pumping test data indicated a storativity of 0.0342. Their findings revealed that rainfall contributes approximately 35% to GW recharge, with a lag time of one month between the rainfall events and corresponding GW level fluctuations.

Sun et al. (2013) applied the Rainfall Infiltration Breakthrough (RIB) model, a modified of the revised CRD method, to estimate GW recharge from rainfall percolating through the unsaturated zone to the water table in two research sites in western coastal South Africa. These sites represent two distinct geological settings: (1) The coastal plain sand aquifer with diffuse recharge in Riverlands Nature Reserve (Western Cape, South Africa), and (2) the Table Mountain Group aquifer (TMG) with localized recharge in Oudebosch catchment of Kogelberg Nature Reserve (Western Cape, South Africa). The storativity of the aquifers ranged from 0.05 to 0.15 for fine to medium sand cover, with water table depths between 1.6 m and 3.5 m. GW recharge estimates varied between 16%–47% at the daily scale and 9.3%–27.8% at the monthly scale in Riverlands, while in Oudebosch, recharge was estimated at 51.5% of the Mean Annual Precipitation (MAP) at the daily scale and 15.7% at the monthly scale.

Several open questions remain regarding the applicability of the CRD method, particularly for deep aquifers (Xu and Van Tonder, 2001) and under different climatic and hydrogeological conditions (Sun et al. 2013). This study aims to evaluate the applicability of the CRD method under tropical climatic conditions, distinct from the arid and semi-arid settings in which it has been traditionally applied. Additionally, it seeks to assess the method's suitability for deep aquifers influenced by vertical inter-aquifer flow through semi-pervious aquitards and rainfall percolation through the surface aquitard in the Vietnamese

Mekong Delta (Soc Trang Province), located in the southernmost region of Vietnam. The reliability of the method for deep aquifers in a tropical climate will be assessed by analyzing the correlation between observed GW levels and those derived from the CRD model.

1 Cumulative Rainfall Departure method (CRD)

1.1 Method description

The revised CRD method establishes a relationship between GW level fluctuations and the departure of rainfall from the mean precipitation over a preceding period. It is defined as follows (Xu and Van Tonder, 2001):

$$ {}_{t}^{1}CRD_i = \sum_{n=1}^{i} R_n - \left(2 - \frac{1}{R_{av} i} \sum_{n=1}^{i} R_n\right) \sum_{n=1}^{i} R_t; \quad (n = 1,\ 2,\ 3 \cdots N) \tag{1} $$

Where: N is the total length of rainfall series; R_i is the rainfall amount at i^{th} time scale (daily, monthly or annually); R_{av} is the mean precipitation of the whole time series; R_t is a threshold value representing the boundary conditions.

A linear relationship is assumed between the Cumulative Rainfall Departure (CRD_i) and the GW level change (Δh_i) over the ith time interval:

$$ \Delta h_i = \frac{r}{S}\left({}_{t}^{1}CRD_i\right); \ (i = 0,\ 1,\ 2,\ 3 \cdots N) \tag{2} $$

Where: Δh_i is the change in GW level during the ith time interval; r represents the fraction of cumulative rainfall departure that contributes to recharge; S is the aquifer storativity (i.e. the aquifer storage coefficient S^* for confined aquifer or the specific yield μ for the unconfined aquifer).

Therefore, Eq. (2) can be used to estimate the ratio of the aquifer recharge to the aquifer storativity by performing a regression analysis between CRD_i and Δh_i.

In case where natural aquifer discharge and/or pumping significantly influence GW level fluctuations, the following equation is used instead of Eq. (2):

$$ \Delta h_i = \frac{r}{S}\left({}_{t}^{1}CRD_i\right) - \frac{Q_{out,i}}{AS}; \ (i = 0,\ 1,\ 2,\ 3 \cdots N) \tag{3} $$

Where: Q_{outi} is the total natural aquifer discharge and groundwater abstraction during the ith time interval; A is the area influenced by aquifer discharge, pumping, or artificial recharge.

If the rainfall departure is positive, the GW water level will rise, and if it is negative, the GW level will decline. However, as long as recharge exceeds discharge, the GW level may continue to rise even when the rainfall departure is negative.

1.2 Determination of R_t values

According to Xu and Van Tonder (2001), the threshold value of R_t determines the nature of the aquifer system. A value of R_t=0 represents a closed aquifer system, implying that recharge at a given time step i depends only on preceding rainfall events. Conversely, a value of R_t=R_{av} represents an open system, which may be regulated by spring flow. The values of both r and R_t are determined during the simulation process.

In the current study, values of R_t significantly greater than R_{av} have been observed. This phenomenon is further examined and discussed below.

To address R_t, let us assume that rainfall is the sole recharge source and there is no additional discharge. In this scenario, Eq. (1) and Eq. (2) can be rewritten as follows:

$$ r = \frac{S\,\Delta h_i}{\sum_{n=1}^{i} R_n - \left(2 - \frac{1}{R_{av} i} \sum_{n=1}^{i} R_n\right) \sum_{n=1}^{i} R_t}; \quad (n = 1,\ 2,\ 3 \cdots N) \tag{4} $$

Case 1: R_t=0

$$ \Delta h_i = \frac{r}{S} \sum_{n=1}^{i} R_n; \ (n = 1,\ 2,\ 3 \cdots N) $$

which implies that Δh_i increases over time as $\sum_{n=1}^{i} R_n$ increases with n.

Case 2: R_t=R_{av}

If rainfall events R_i do not exhibit a trend, then the cumulative rainfall average will converge to R_{av} (Xu and Van Tonder, 2001):

$$ \Delta h_i = \frac{r}{S}\left[\sum_{n=1}^{i} R_n - \left(2 - \frac{1}{R_{av} i} \sum_{n=1}^{i} R_n\right) \sum_{n=1}^{i} R_{av}\right] = \frac{r}{S}\left(\sum_{n=1}^{i} R_n - \sum_{n=1}^{i} R_{av}\right); \ (n = 1,\ 2,\ 3 \cdots N) \tag{5} $$

Eq.(5) is the CRD formula proposed by (Bredenkamp et al. 1995) with k=1, meaning there is no pumping or natural discharge:

$$ {}_{t}^{i}CRD_i = \sum_{n=1}^{i} R_n - k \sum_{n=1}^{i} R_{av}; \ (n = 1,\ 2,\ 3 \cdots N) \tag{6} $$

Case 3: $R_t > R_{av}$

To account for the net effect of pumping and/or natural outflow $Q_{out,i}$ in Eq. 3, we consider using a threshold value $R_t > R_{av}$, particularly since actual *CRD* analysis has shown a stable water level fluctuation when using $R_t = R_{av}$. In this case:

$$
\begin{aligned}
&{}_t^1CRD_i(R_{av}) - {}_t^1CRD_i(R_t) = \\
&\left[\sum_{n=1}^{i} R_n - \left(2 - \frac{1}{R_{av} i}\sum_{n=1}^{i} R_n\right)\sum_{n=1}^{i} R_{av}\right] - \\
&\left[\sum_{n=1}^{i} R_n - \left(2 - \frac{1}{R_{av} i}\sum_{n=1}^{i} R_n\right)\sum_{n=1}^{i} R_t\right] = \\
&\left(2 - \frac{1}{R_{av} i}\sum_{n=1}^{i} R_n\right)\left(\sum_{n=1}^{i} R_t - \sum_{n=1}^{i} R_{av}\right); \\
&(n = 1,\ 2,\ 3 \cdots N) \qquad (7)
\end{aligned}
$$

Where: ${}_t^1CRD_i(R_{av}), {}_t^1CRD_i(R_t)$ are *CRD* values determined with $R_t = R_{av}$ and $R_t > R_{av}$, respectively.

Therefore, the GW level drawdown (Δs_i) due to the net effect of pumping and/or natural discharge can be expressed as:

$$
\Delta s_i = \frac{r}{S}\left(2 - \frac{1}{R_{av} i}\sum_{n=1}^{i} R_n\right)\left(\sum_{n=1}^{i} R_t - \sum_{n=1}^{i} R_{av}\right); \quad (n = 1,\ 2,\ 3 \cdots N) \qquad (8)
$$

2 Application of the CRD method to the study area

The study area is Soc Trang Province, covering an area of 3,332 km^2, located in the southernmost region of Vietnam's Mekong Delta, at the downstream end of the Mekong River basin delta (Fig. 1). The Vietnamese Mekong Delta includes Can Tho city and 12 provinces: Long An, Tien Giang, Ben Tre, Vinh Long, Tra Vinh, Hau Giang, Soc Trang, Dong Thap, An Giang, Kien Giang, Bac Lieu, and Ca Mau. The total area of the Mekong Delta is 40,816 km², with a population approaching 18 million (Phuong et al. 2019).

2.1 General conditions of the study area

Soc Trang province features a relatively low and flat terrain, characterized by flat land interspersed with depressions and sand dunes. The ground surface elevation varies between 0.2–2 meters above sea level (DWRPIS, 2018). The province is served by a relatively dense network of rivers and canals, with the Hau River being the most signifi-

Fig. 1 Location map of Southern Vietnam, Vietnamese Mekong delta, study area and GW monitoring wells

cant, flowing along the eastern border of the province for about 60 km. Rivers and canals in Soc Trang are affected by an irregular semi-diurnal tide regime. The province also has 72 km of coastline. The hydrological regime of the study area is influenced by the ocean tides, leading to significant saltwater intrusion in the local rivers and canals (DWRPIS, 2018).

Soc Trang is located in a tropical climate zone influenced by monsoons, which divide the year into dry and rainy seasons. The rainy season lasts from May to October, while the dry season extends from November to April. The average annual temperature ranges from 27.0°C to 27.4°C, and the area is rarely impacted by storms or floods. The total annual sunshine hours range from 2,326 hours to 2,612 hours. The average annual rainfall is between 1,540 mm and 1,893 mm, with a significant seasonal variation - approximately 90% of the total rainfall occurs during the rainy season (DWRPIS, 2018).

2.2 About the GW resources of the area

GW is a critical freshwater resource for residents of the Vietnamese Mekong Delta, especially during the dry seasons when surface water quality deteriorates throughout most of the delta (Dinh Phuc, 2008; Eastham et al. 2008; IDE-Cambodia, 2009; Wagner et al. 2012). GW in the region is exploited via dug wells, small-scale household tube wells, and medium to large-scale central supply wells, which were constructed as part of the Rural Clean Water Supply Program (IUCN, 2011; Nuber and Stolpe, 2008; Thomas and Harro, 2008). In the Vietnamese Mekong Delta, GW accounts for 60% to 100% of drinking water supply. In addition, this resource is crucial for irrigation and aquaculture, particularly in the coastal areas (Bui et al. 2015).

However, excessive GW exploitation, especially over-exploitation, has causes land subsidence, which poses a flood risk in the coastal areas of the Delta. The average annual decline of GW is approximately 0.3 m, with land subsidence occurring at an average annual rate of 1.6 cm per year (Erban et al. 2014). From 1991 to 2015, the Delta sank by an average of 18 cm, with rates in 2016 ranging from 1.1 cm/year to 2.5 cm/year due to GW withdrawal (Minderhoud et al. 2017). Projections presented by Minderhoud et al. (2020) using a 3D hydrogeological model with a coupled geotechnical module forecast that, if GW extraction continues at the current rate, extraction-induced subsidence could inundate the Vietnamese Mekong Delta before the end of the century. The combined effects of global sea-level rise (Eslami et al. 2021), GW abstraction and the resultant subsidence further exacerbate saltwater intrusion (Erban et al. 2014; Hori, 2000).

To ensure the sustainable future utilization of GW resources in the Vietnamese Mekong Delta, it is essential to determine the annual renewable component of GW, which can serve as the safe yield of GW. A significant components of this renewable reserves is derived from rainwater recharge. With an average annual rainfall exceeding 1,500 mm, and the region's surface soil comprising permeable materials such as sand and silty sand, as well as less permeable formations like silt and semipermeable clay, the GW dynamic reserve from rainfall is considerable.

2.3 Hydrological conditions of the study area

The hydrogeological conditions of the Mekong Delta, and Soc Trang province in particular (Fig. 1), are characterized by seven aquifers and seven semi-pervious layers (Fig. 2) (BGR, 2017; DWRPIS, 2018).

Holocene porous aquifer (*qh*)

The Holocene aquifer (*qh*) consists of layers of fine sand and blackish gray silty sand, located at the bottom of the oceanic sediments cross-section that belongs to the Hau Giang formation ($mQ_2^{1\text{-}2}hg$). The upper portion of the aquifer is typically covered by silty clay and clay layers, which belong to the very poor water-bearing formations of the Holocene age. This aquifer often lies above the very poor water-bearing formation Q_1^3. The thickness of the Holocene aquifer ranges from several meters to over 30 m, with an average of around 20 m. While the Holocene aquifer is exposed to the ground surface in some locations, it is predominantly underlain by the Holocene semi-pervious layer (Q_2).

Aquifer storativity (S), which is the product of the specific storage of the aquifer material (S_s) and aquifer thickness, is a critical parameter in determining rainwater recharge in the aquifer, as discussed in Section 2.1. The specific storage of the aquifer is determined by the water unit weight, compressibility of the water and aquifer material, and total porosity. Water at 25°C has a compressibility of 4.6×10^{-10} m^2/N, while fine sand to medium sand with grits or gravels has a compressibility of approximately 1.3×10^{-8} m^2/N (Fetter,

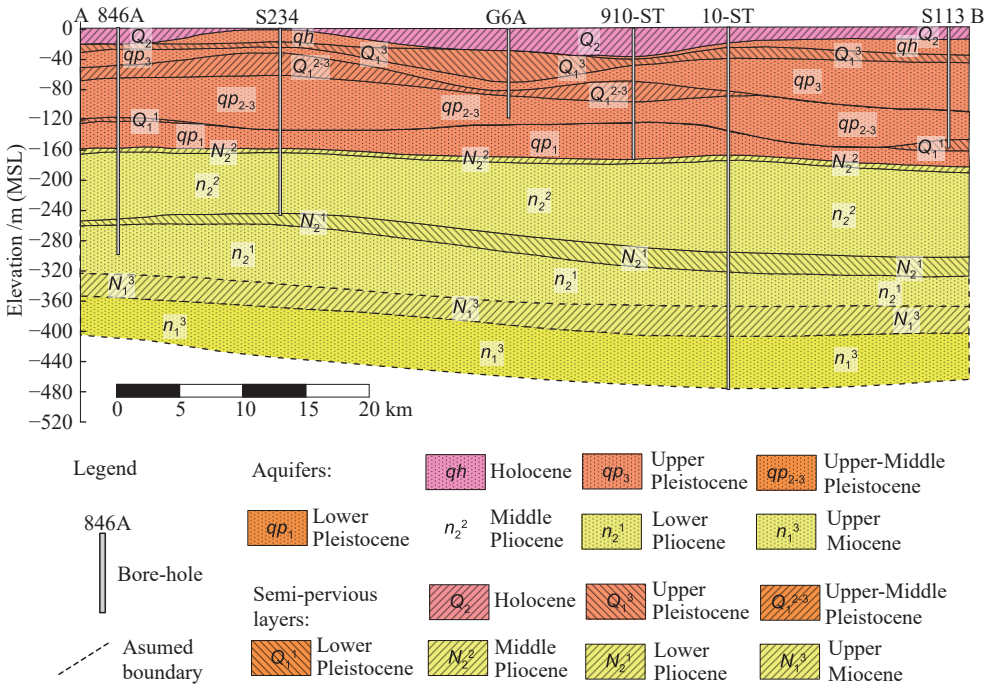

Fig. 2 Hydrogeological cross-section along Line AB

2001). With the porosity of the Holocene and Pleistocene aquifers estimated to be around 0.25 (DWRPIS, 2018), the specific storge of the aquifers material is around 0.00013/m. Therefore, the storativity of the Holocene aquifer is calculated to be 0.0026.

The nearest GW monitoring well (Q1770) in the *qh* aquifer is located in Ca Mau province (Fig. 1), approximately 97 km southwest of Soc Trang city.

Upper Pleistocene porous aquifer (qp_3)

The Upper Pleistocene aquifer (qp_3) consists of layers of ash-gray, blue-gray, yellow-gray coarse grain sediments from the Long My formation (mQ_1^3lm). These sediments are predominantly fine sand and fine to medium-sized sand, with a small amount of gravel, and contain greenish grey and whitish-grey shells. This formation is found throughout Soc Trang, with a thickness ranging from a few meters to 60 m (average 30 m). The depth of the aquifer surface varies from 24 m to 95 m (average 50 m) and the depth of the bottom ranges from 30 m to 125 m (average 71 m). The Upper Pleistocene aquifer is underlain by the Upper Pleistocene semi-pervious layer (Q_1^3) of the Long My formation and lies above the Middle-Upper Pleistocene semi-pervious layer ($Q_1^{2\text{-}3}$) of the Long Toan formation ($mQ_1^{2\text{-}3}lt$). With an average thickness of 30 m, the storativity of the qp_3 aquifer is calculated to be 0.0039.

The GW monitoring well Q4090, located in Soc Trang city (Fig. 1), monitors the qp_3, $qp_{2\text{-}3}$, and qp_1 aquifers.

Upper Middle-Upper Pleistocene porous aquifer ($qp_{2\text{-}3}$)

The Middle-Upper Pleistocene aquifer ($qp_{2\text{-}3}$) consists of layers of ash-gray, blue-gray, and yellow-gray coarse grains from the lower basement of Long Toan formation ($mQ_1^{2\text{-}3}lt$). The $qp_{2\text{-}3}$ aquifer is distributed across the entire Soc Trang province, located beneath the very poor water-bearing layer of the Long Toan formations ($mQ_1^{2\text{-}3}lt$) and above the very poor water-bearing layer of the Binh Minh formation (m,amQ_1^1bm). The depth of the aquifer's surface ranges from 54 m to 137 m (average 83 m), while the bottom depth varies from 92 m to 175 m (average 131 m). The aquifer thickness fluctuates from 7 m to 81 m (average 50 m). Like the *qh* and qp_3 aquifers, the storativity of the aquifer $qp_{2\text{-}3}$, with an average thickness of 50 m, is calculated to be 0.0065. The GW monitoring well Q5980, located in the Soc Trang city, monitors the $qp_{2\text{-}3}$ aquifer (Fig. 1).

Lower Pleistocene porous aquifer (qp_1)

The Lower Pleistocene aquifer (qp_1) consists of layers of dark-gray, ash-gray, fine to coarse grains found at the bottom of Binh Minh formation (m,amQ_1^1bm), interspersed with thin lenses of clay, silt clay, and silt sand. The prominent lithological components are primarily fine to coarse sand mixed with some gravel, with some relatively thick aquiclude lenses described in the cross-sections. The aquifer is distributed across the entire Soc Trang Province. The surface of the aquifer lies at depths ranging from 110 m to 192 m (average 145

m), while the bottom depth ranges from 146 m to 250 m (average 187 m). It is underlain by the Lower Binh Minh formation (Q_1^1bm) semi-pervious layer (Q_1^1) and lies above the Middle Pliocene (Nam Can Formation - N_2^2nc) semi-pervious layer (N_2^2). The aquifer's thickness ranges from 6 m to 80 m (average 40 m). Similarly to the *qh*, qp_3 and $qp_{2\text{-}3}$ aquifers, the storativity of qp_1 aquifer is 0.0052. The GW monitoring well Q4090 monitors the qp_1 aquifer (Fig. 1).

Middle Pliocene porous aquifer (n_2^2)

The Middle Pliocene aquifer (n_2^2) consists of layers of blue-gray, light yellow coarse grain sand mixed with small amounts of gravel, found at the bottom of the Nam Can formation (a,amN_2^2nc). The aquifer is covered by very poor water-bearing upper Nam Can formations (N_2^2nc) and lies above the very poor water-bearing part of the Lower Can Tho formations (N_2^1ct). The aquifer is distributed across the entire Soc Trang province. The surface of the aquifer is found at depths between 156 m and 273 m (average 201 m), while the bottom is at depths ranging from 186 m to 307 (average 246 m). The aquifer thickness ranges from 18 m to 123 m (average 78 m). Similar to the other aquifers, with the average thickness, the storativity is estimated to be 0.0125.

Lower Pliocene porous aquifer (n_2^1)

The Lower Pliocene aquifer (n_2^1) consists of layers of ash-gray, blue-gray, light gray fine to coarse sand, mixed with some clay and, in some places, with gravels. It is interbedded with layers of gray, ash-gray silty sand and silt. This aquifer is underlain by the Lower Pliocene semi-pervious layer (N_2^1) and lies above the Upper Miocene (Phung Hiep Formation - N_1^3ph) semi-pervious layer (N_1^3). The n_2^1 aquifer ranges from 31 m to 45 m, with an average of 39 m. Similar to other aquifers, the storativity of the n_2^2 aquifer is estimated to be 0.0085.

Upper Miocene porous aquifer (n_1^3)

The Upper Miocene aquifer (n_1^3) consists of layers of fine to coarse sand, sometimes interbedded with layers of silt. It is underlain by the Upper Miocene semi-pervious layer (N_1^3). The thickness of the n_1^3 aquifer ranges from 15 m to 83 m, with an average of 67 m. The sotrativity of the n_2^2 aquifer is estimated to be 0.0125.

Semi-pervious layers

The semi-pervious layers in Soc Trang Province, as previously mentioned, have the following lithological characteristics and the thicknesses (DWRPIS, 2018).

Semi-pervious Holocene layer Q_2: The thickness ranges from 1 m to 57 m, with an average of 27 m. It consists of ash-gray, dark-gray, yellow clayey silt, and silt interbedded with lenses of fine sand.

Semi-pervious Upper Pleistocene layer Q_1^3: The thickness ranges from 2 m to 54 m, with an average of 22 m. It consists of ash-gray, dark-gray, blue-gray silty clay, silt, silty sand, occasionally interbedded with lenses of fine sand.

Semi-pervious Upper-Middle Pleistocene layer $Q_1^{2\text{-}3}$: The thickness ranges from 2 m to 43 m, with an average of 15 m. It consists of ash-gray, blue-gray laterite clay, silt, and clayey silt.

Semi-pervious Lower Pleistocene layer Q_1^1: The thickness ranges from 2 m to 37 m, with an average of 12 m. It consists of blue-gray, dark-gray, red-gray laterite clay, silty clay, silt, sometimes interbedded with fine sand mixed with much silt.

Semi-pervious Middle Pliocene layer N_2^2: The thickness ranges from 3 m to 96 m, with average of 24 m. It consists of blue-gray, light-gray, and red-gray clay.

Semi-pervious Lower Pliocene layer N_2^1: The thickness ranges from 22 m to 29 m, with average of 25 m. It consists of blue-gray, light-gray, dark-gray, yellow-gray clay, silty clay, clayey silt with laterite grits.

Semi-pervious Upper Miocene layer N_1^3: This layer consists primarily of tight silt and clay and has a thickness ranging from 19 m to 73 m, with an average of 46 m.

The semi-pervious layers exhibit low hydraulic conductivity, ranging from 10^{-7} m/day to 10^{-4} m/day (DWRPIS, 2018). The aforementioned aquifers and aquitards are distributed beneath the East Sea within the Vietnamese Mekong Delta and extend to the Kingdom of Cambodia and the Lao People's Democratic Republic.

According to DWRPIS (2018), the recharge of the aquifers is exclusively from rainfall: Rainwater infiltrates to recharge the Holocene aquifer *qh*, which in turn recharges the Upper Pleistocene aquifer, and so on.

The GW levels of the aquifers follow a descending sequence from the topmost aquifer (the Holocene aquifer, which has the lowest GW level) to the lowest Quaternary aquifer (the Lower Pleistocene porous aquifer, which has the highest GW level). The GW levels in the Holocene aquifer, as observed in the monitoring well Q1770 in Ca Mau city (97 km southwest of monitoring well Q4090), and in the Lower Pleistocene aquifer in the monitoring well Q5980 in Soc Trang city are shown in Fig. 3. Additionally, the GW levels in the Upper Pleistocene aquifer and the Low-Middle Pleistocene aquifer, as recorded in the monitoring well

Q5970 in Bac Lieu City (42 km southwest of monitoring well Q4090), are shown in Fig. 4.

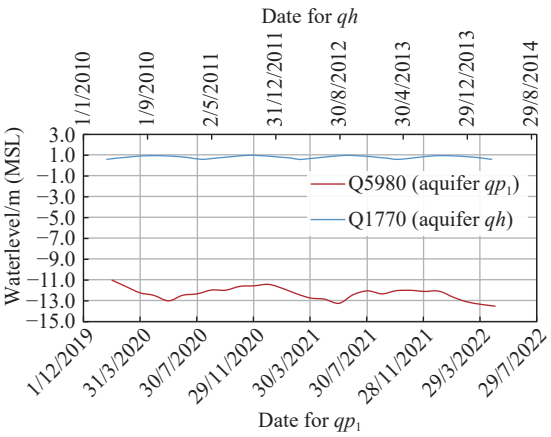

Fig. 3 GW levels of aquifers *qh* (monitoring well Q1770) and qp_1 (monitoring well Q5980)

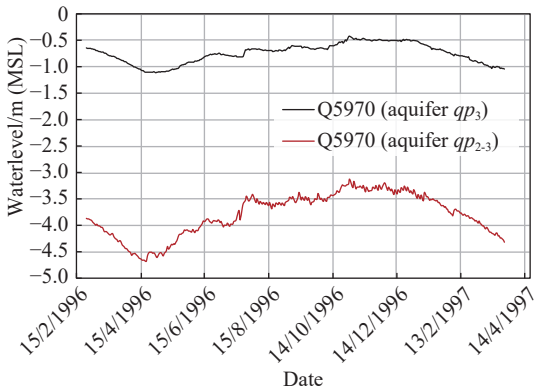

Fig. 4 GW levels of qp_3 and $qp_{2\text{-}3}$ aquifer, monitored by monitoring well Q5970

2.4 Capability of the CRD method in addressing deep vertical inter-aquifer flow in the study area

The GW levels of the qp_3, qp_1 and n_2^2 aquifers have been monitored since 2010, during which time GW abstraction has been occurring in the context of the country's high economic activity. The fluctuations in the water levels of the aquifers within the multi-aquifer system in the study area are synchronized with one another (Fig. 5), and Pearson correlation analysis has shown high degree of correlation, with coefficients greater than 0.993, between the monthly water levels of aquifers qp_3, qp_1, and n_2^2 (Fig. 6).

This correlation suggests that an increase in the water level of the qp_3 aquifer induces vertical GW flow from qp_3 to $qp_{2\text{-}3}$, from $qp_{2\text{-}3}$ to qp_1, and from qp_1 to n_2^2 through the semi-pervious layers. The vertical flow rates, which effectively recharge the

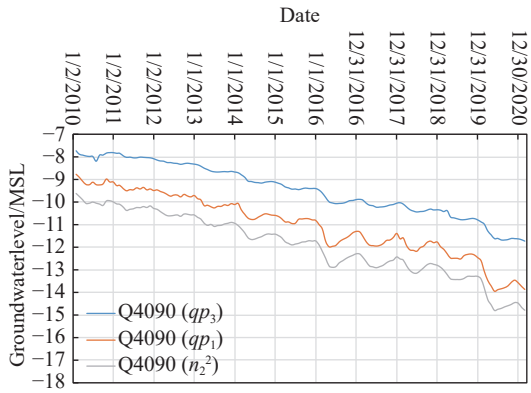

Fig. 5 GW levels of qp_3, qp_1, and n_2^2 aquifers from 1 Jan. 2010 to 31 Dec. 2023, monitored by monitoring well Q4090 in Soc Trang city

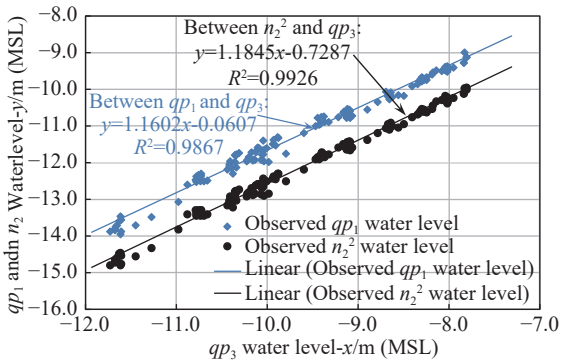

Fig. 6 Correlation between 2010-2023 GW levels of qp_3, $qp_{2\text{-}3}$ and n_2^2 in monitoring well Q4090 in Soc Trang City

aquifers, can be estimated using Darcy law. These vertical flow rates may be calibrated by assuming that the rate is determined by the difference in water levels between the aquifers and the hydraulic conductivities of the semi-pervious layers.

The relationship between rainfall and GW levels in the uppermost aquifer, *qh*, is an important aspect of understanding GW recharge. The *qh* aquifer is recharged by rainfall through infiltration, which occurs either through the unsaturated or saturated zone above it. The fluctuation in the water level of the uppermost aquifer is directly influenced by the rate of this rainfall infiltration. In this study, rain-water infiltration occurs through the Holocene semi-pervious silty layer (Q_2), which has an average thickness of 28 m.

The lag time, or the delay before the groundwater level responds to rainfall, is defined as the time it takes for the wetting front to reach the bottom of the semi-pervious layer. The CRD method is capable of analyzing this lag time by comparing time series of CRD-simulated water level fluctuations with monitored GW level.

For this study, a lag time of one month is

initially used in the CRD model: The analysis uses the data series of monthly rainfall from 2010 to 2020 in Soc Trang City (NHMS, 2024) and the daily monitored GW levels during the same period (NAWAPI, 2024) at the end of each month.

2.5 The application results

The GW level monitoring in the study area has faced some challenges, particularly in terms of inconsistent installation of monitoring wells across different aquifers and periods of uncorrected data. Therefore, specific time periods for each aquifer were selected for the analysis to mitigate these issues.

Fig. 7, Fig. 8 and Fig. 9 present the CRD-simulated monthly Water Level (WL) fluctuations and the observed monthly fluctuations for the qp_3, qp_1, and n_2^2 aquifers (NAWAPI, 2024), respectively. The results indicate a relatively high correlation between the simulated and observed water levels, with Pearson correlation coefficient ranging from 0.995 to 0.997. Table 1 summarizes the key analysis results.

Since there are no available monitored water level data of the Middle Pleistocene aquifer ($qp_{2\text{-}3}$), estimates must be made base on the characteristics of the aquifer and the overlying semi-pervious layer. The vertical recharge rate is assumed to be inversely proportional to the thickness of the overlying semi-pervious layer, with the hydraulic conductivity of these layers assumed to be approximately constant.

For the qp_1 aquifer, the thicknesses of the over-

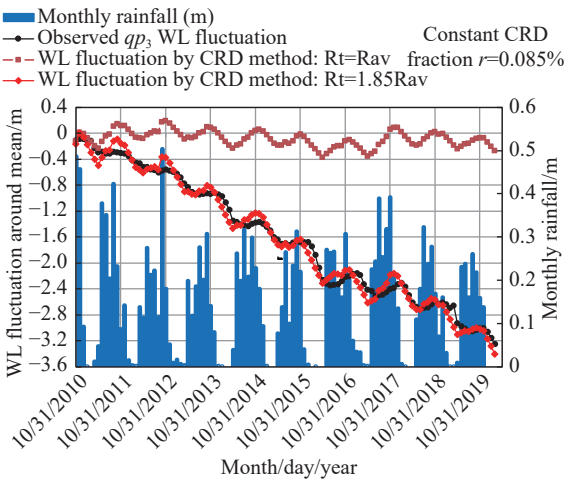

Fig. 7 Observed and CRD-simulated WL fluctuations of qp_3 aquifer during Oct. 2010-Apr. 2020

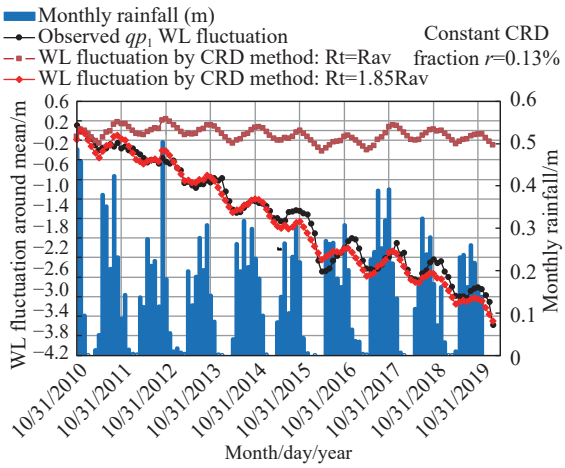

Fig. 8 Observed and CRD-simulated WL fluctuations of qp_1 aquifer during Oct. 2010-Apr. 2020

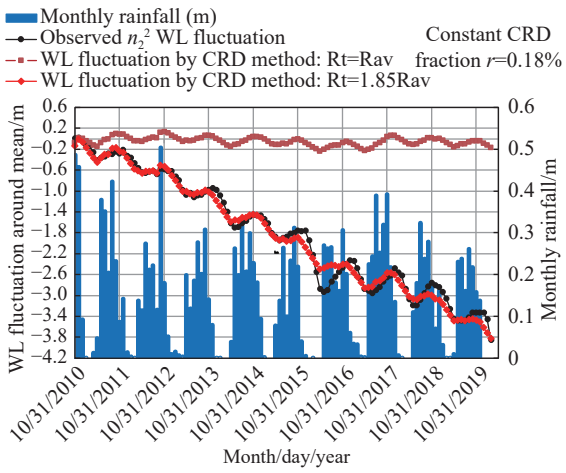

Fig. 9 Observed and CRD-simulated WL fluctuations of n_2^2 aquifer during Oct. 2010-Apr. 2020

Table 1 Determined net recharge values using the CRD method

Aquifer	R_t	Pearson correlation coef. (r)	Annual rainfall/mm	Percentage of rainfall/%	Annual net recharge/mm
qp_3	1.25	0.997	1,555	0.085	1.32
$qp_{2\text{-}3}$			1,555	0.104 (estimated)	1.62
qp_1	1.20	0.995	1,555	0.130	2.02
n_2^2	2.50	0.996	1,555	0.180	2.80
			Average: 1,555	Total: 0.499	Total: 7.76
			The whole Soc Trang area of 3,332 km^2:		25.86×10^6 m^3/year
					70,850 m^3/day

lying semi-pervious layers is 12 m, and the average rate is 0.13% of the rainfall. Similarly, for the $qp_{2\text{-}3}$ aquifer, which has a 15 m thickness overlying semi-pervious layer, the recharge rate can be estimated to be 0.104% of the rainfall (Table 1).

The fractions of CRD for aquifers qp_3, $qp_{2\text{-}3}$, qp_1 and n_2^2 are 0.085%, 0.104%, 0.130% and 0.180%, respectively, which sum up to a total of 0.499% of the rainfall. Although these fractions are relatively small, they indicate the contribution of rainfall to groundwater recharge. The total recharge from rainfall across the entire Soc Trang province is estimated at 25.86 million m^3 annually, or approximately 70,850 m^3/day.

In comparison, the current GW abstraction from the Quaternary aquifers is about 101,000 m^3/day, and the estimated domestic water demand for 2030 is expected to rise to 153,000 m^3/day (Nhan et al. 2019). Therefore, the recharge from rainfall can only meet approximately 70% of the current groundwater abstraction and about 46% of the projected 2030 abstraction. The remaining 30% and 54% of the current and projected abstractions, respectively, are sourced from unsustainble groundwater mining.

3 Discussions

The CRD method, originally developed for arid and semi-arid with shallow aquifers, has been successfully applied to deep aquifers in this study. The validity of the CRD method for deep aquifers can be supported by Darcy law, which describes the vertical inter-aquifer flow in terms of the difference in water level between the upper and lower aquifers, the thickness, and hydraulic conductivity of the semi-pervious layer between them. The flow velocity of vertical flow in deep wells has been validated by Wang et al. (2013), who used both field measurements and numerical simulations.

The results of this study show that the CRD-simulated GW levels for two Quaternary aquifers and one Neogene fractured aquifer are tightly correlated with monthly rainfall. This suggests that the preceding month's rainfall directly influence the fluctuation of GW levels at the end of the month.

The authors of the CRD method proposed that, for an open aquifer system, the threshold value (R_t) representing the boundary conditions is equal to the average rainfall (R_{av}). However, the present study reveals that R_t equals $1.85R_{av}$ for all the considered aquifers, indicating that the GW level decrease due to the abstraction corresponds to $0.85R_{av}$ of the total R_t ($1.85R_{av}$). This discrepancy offers an intriguing topic for further investigation.

There have been very few studies on GW recharge from rainfall in the study area. Van Canh et al. (2018), using stable isotopes (δ^2H and δ^{18}O), found that surface water, including rainwater, weakly recharges deep aquifers in the Vietnamese Mekong Delta. This aligns with the findings of the present study. Huy Dong (2020) estimated that the GW recharge from rainfall on coastal sand dunes in the Southern Hau River area of Soc Trang province is 24.4% of the rainfall, which is nearly 50 times the total recharge calculated for the four aquifer (qp_3, $qp_{2\text{-}3}$, qp_1 and n_2^2) in this study.

Tu et al. (2022) used time-series tracer data (δ^{18}O, δ^2H, major ions and ^{3}H) to estimate GW recharge to the Pleistocene aquifer in the Vietnamese Mekong Delta, with recharge rates ranging from less than 5% up to 16% of rainfall. However, the study did not provide explicit expression for the GW recharge estimate using δ^{18}O, and the δ^{18}O time series at two locations were contradictory. Given this, the most likely recharge value would be less than 5% which is approximately 10 times higher than the total recharge values for the four aquifers (qp_3, $qp_{2\text{-}3}$, qp_1 and n_2^2) obtained in the present study.

Lertsirivorakul et al. (2023), using the water table fluctuation method, estimated the average GW recharge for the Upper Pleistocene aquifer (qp_3) in Soc Trang Province in 2005, 2009, 2013 and 2020 to be 0.71% of the rainfall, assuming an aquifer storage coefficient of 0.0039 used in this study. This value is about 8 times the recharge of aquifer qp_3 obtained in the present study.

Therefore, the estimate of GW recharge from the rainfall in this study is comparable to the values found in the works of Van Canh et al. (2018), Tu et al. (2022) and Lertsirivorakul et al. (2023). The obtained values are within the same order of magnitude as specified by Kinzelbach and Aeschbach (2002) with the present study yielding the lowest estimate.

Given that rainfall contributes only a limited amount of recharge to deep aquifers, which is consistent with the findings of this study, and due to uncertainties in the hydrological cycle, it is essential to explore other methods to validate the results obtained by applying the CRD method in this study.

4 Conclusion

The CRD method, originally developed for use in arid and semi-arid regions with shallow aquifers,

was successfully applied in this study to two deep Quaternary aquifers and one Neogene fractured aquifer in Soc Trang Province, located in the tropical climate of the Vietnamese Mekong Delta. The results demonstrate that the CRD-simulated GW levels in these aquifers exihibit a strong correlation with monthly rainfall, indicating that rainfall from the preceding month influence water level fluctuations at the end of the month.

The study estimates that GW recharge from rainfall in the Upper Pleistocene, Middle Pleistocene, Lower Pleistocene and Middle Pliocene aquifers is very small, about 0.5% of the total rainfall, which accounts for approximately 70% of the current GW abstraction in the province. Since the importance of GW as a freshwater source in the area, an enhanced GW recharge program using surface water and rainwater is strongly recommended.

While the authors of the CRD method suggested that the threshold value representing the boundary conditions (R_t) for an open aquifer system equals the average rainfall (R_{av}), this study found that R_t is 1.85 times R_{av} for all considered aquifers. It means that, under the assumption that the aquifers considered in this study are open, the decrease in GW levels due to abstraction corresponds to 0.85 times the average rainfall (R_{av}) of the total threshold value (R_t =1.85R_{av}). This discrepancy offers an intriguing topic for further investigation.

The application of the CRD method in this study also demonstrated its ability to simulate seasonal GW fluctuations with high accuracy when compared to long-term monitored GW levels, i.e. about ten years in this study. This is noteworthy because many existing recharge estimation methods struggle to achieve such a close match over extended timeframe.

Acknowledgments

This paper was completed as part of the Research project (CT.2022.01.MDA.02): "Research and evaluation of the role of the hydrogeological and engineering geological factors in the change of the flows and of the coastal area of the Hau River mouth in the southwest region of Vietnam", funded by the Vietnam Ministry of Education and Training. The GW monitoring data used in this study were sourced from BIGDATA, NAWAPI.

References

Adams S, Titus R, Xu, Y. 2003. Groundwater recharge assessment of the basement aquifers of central Namaqualand University of the Western Cape Cape Town. Available on https://www.wrc.org.za/wp-content/uploads/mdocs/1093-1-041.pdf

Baalousha H. 2005. Using CRD method for quantification of groundwater recharge in the Gaza Strip, Palestine. Environmental Geology, 48: 889–900. DOI：10.1007/s00254-005-0027-x.

BGR (Bundesanstalt für Geowissenschaften und Rohstoffe - Organisation of the Federal Institute for Geosciences and Natural Resources). 2017. German Technical Cooperation with Vietnam - Improvement of Groundwater Protection in Vietnam: Final Report of the IGPVN activities and achievements in Soc Trang, Proposal of recommendations and measures for water resources management in Soc Trang.

Bredenkamp D, Botha L, Van Tonder G. et al. 1995. Manual on quantitative estimation of groundwater recharge and aquifer storativity: Based on practical hydrological methods. Water Research Commission.

Bui T, Lam D, Van L, et al. 2015. Groundwater issues and hydrogeological survey of the Mekong River basin in Vietnam in the document TH/SC/15-02 "Current status and issues of groundwater in the Mekong river basin", Chief Editors: Kyoochul Ha, Nguyen Thi Minh Ngoc, Eunhee Lee, Ramasamy Jayakumar. Published by Korea Institute of Geoscience and Mineral Resources (KIGAM) CCOP Technical Secretariat UNESCO Bangkok Office Coordinating Committee For Geoscience Programmes In East And Southeast Asia, 93–121.

Cheng YP, Zhang FW, Hua D, et al. 2024. Groundwater and environmental challenges in Asia. Journal of Groundwater Science and Engineering, 12(2): 223–236. DOI：10.26599/JGSE.2024.9280017.

Dinh Phuc D. 2008. General on groundwater resources. Department of Water Resources Management, Water sector review project. (in Vietnamese)

Djellali M, Guefaïfia O, Fehdi C, et al. 2023. Assessing the impact of artificial recharge on groundwater in an over-exploited aquifer: A case study in the Cheria Basin, North-East of

Algeria. Journal of Groundwater Science and Engineering, 11(263): 277. DOI：10.26599/JGSE.2023.9280022.

DWRPIS (Division for Water Resources Planning and Investigation for the South of Vietnam). 2018. Compilation and edition of Vietnam groundwater resources mapping, Southern Vietnam Plain, scale 1: 200, 000, Soc Trang Province. (in Vietnamese)

Eastham J, Mpelasoka F, Mainuddin M, et al. 2008. Mekong river basin water resources assessment: Impacts of climate change. In: CSIRO: Water for a healthy country National Research Flagship Canberra.

Erban LE, Gorelick SM, Zebker HA. 2014. Groundwater extraction, land subsidence, and sea-level rise in the Mekong Delta, Vietnam. Environmental Research Letters, 9(8): 084010. DOI：10.1088/1748-9326/9/8/084010.

Eslami S, Hoekstra P, Kernkamp HWJ, et al. 2021. Dynamics of salt intrusion in the Mekong Delta: results of field observations and integrated coastal–inland modelling. Earth Surface Dynamics, 9(4): 953−976. DOI：10.5194/esurf-9-953-2021.

Eunhee L, Kyoochul H, Nguyen Thi Minh Ngoc, et al. 2017. Groundwater status and associated issues in the Mekong-Lancang River Basin: International collaborations to achieve sustainable groundwater resources. Journal of Groundwater Science and Engineering, 5(1): 1−13. DOI：10.26599/JGSE.2017.9280001.

Fetter CW. 2001. Applied hydrogeology (4th ed.). Prentice Hall.

Hori H. 2000. The Mekong: Environment and development. United Nations University.

Huu Dong T. 2020. Study on the origin of groundwater exploitation reserves in coastal sand dunes in the Southern Hau River region, and proposal of solutions for sustainable groundwater exploitation and use to serve the socio-economic development. Final report of the study project TNMT. 2017.02. 09. (in Vietnamese) Ministry of Natural Resources and Environment.

IDE-Cambodia. 2009. Strategic study of groundwater resources in Prey Veng and Svay Rieng (Phase 1) Final Report. Rural Poverty Reduction Project, Seila Task Force Secretariat, IFAD Loan No. 623- KH, Phnom Penh.

IUCN. 2011. Groundwater in the Mekong Delta. Discussion paper in Mekong Water Dialogues - International Union for Conservation of Nature.

Kinzelbach W, Aeschbach W. 2002. A survey of methods for analysing groundwater recharge in arid and semi-arid regions (Vol. 2). Division of Early Warning and Assessment, United Nations Environment Programme.

Lertsirivorakul R, Vuong BT, Thang CH, et al. 2023. Groundwater recharge in Mekong River Delta: An application of the water-table fluctuation method in the Long Xuyen Quadrangle and the Ca Mau Peninsula. Songklanakarin Journal of Science Technology, 45 (1): 51–58.

Meng RF, Yang HF, Bao XL, et al. 2023. Optimizing groundwater recharge plan in North China Plain to repair shallow groundwater depression zone, China. Journal of Groundwater Science and Engineering, 11(2): 133−145. DOI：10.26599/JGSE.2023.9280012.

Minderhoud P, Middelkoop H, Erkens G, et al. 2020. Groundwater extraction may drown mega-delta: projections of extraction-induced subsidence and elevation of the Mekong delta for the 21st Century. Environmental Research Communications, 2(1): 011005. DOI：10.1088/2515-7620/ab5e21.

Minderhoud PS, Erkens G, Pham V, et al. 2017. Impacts of 25 years of groundwater extraction on subsidence in the Mekong delta, Vietnam. Environmental Research Letters, 12(6): 064006. DOI：10.1088/1748-9326/aa7146.

NAWAPI (National Center for Water Resources Planning and Investigation). 2024. Groundwater monitoring database.

Nhan NT, Trung DT, Anh BTB, et al. 2019. Some results of research and forecasting of groundwater salinization in the coastal zone of Soc Trang Province. Vietnam Journal of Marine Science and Technology, 19(3B): 203−212. DOI：10.15625/1859-3097/19/3B/14526.

NHMS (National Hydro-Meteorological Service of Vietnam). 2024. Rainfall monitoring database.

Nuber T, Stolpe H. 2008. Challenges of the groundwater management in Can Tho City, Vietnam. BGR-Symposium: Sanitation and

groundwater protection.

Parisa K, Ali NZ, Kamran D. 2023. Determining safe yield and mapping water level zoning in groundwater resources of the Neishabour Plain. Journal of Groundwater Science and Engineering, 11(1): 47–54. DOI：10.26599/JGSE.2023.9280005.

Phuong DND, Cuong DK, Dam DT, et al. 2019. Long–term spatio–temporal warming tendency in the Vietnamese Mekong Delta based on observed and high–resolution gridded datasets. European Journal of Climate Change, 1(1): 01–16. DOI：10.34154/2019-ejcc-0101-01-16/euraass.

Rasoulzadeh A, Moosavi S. 2007. Study of groundwater recharge in the Vicinity of Tashk Lake Area. Iranian Journal of Science and Technology, 31(B5): 509.

Shamla R, Marykutty A. 2024. Conventional and futuristic approaches for the computation of groundwater recharge: A comprehensive review. Journal of Groundwater Science and Engineering, 12(4): 428–452. DOI：10.26599/JGSE.2024.9280027.

Sun X, Jovanovic N, Kapangaziwiri E, et al. 2013. Application of the rainfall infiltration breakthrough (RIB) model for groundwater recharge estimation in west coastal South Africa. Water SA, 39(2): 221–230. DOI：10.4314/wsa.v39i2.5.

Tesfaldet YT, Puttiwongrak A, Arpornthip T. 2020. Spatial and temporal variation of groundwater recharge in shallow aquifer in the Thepkasattri of Phuket, Thailand. Journal of Groundwater Science and Engineering, 8(1): 10–19. DOI：10.19637/j.cnki.2305-7068.2020.01.002.

Thomas N, Harro S. 2008. Challenges of the groundwater management in Can Tho City, Vietnam. BGR-Symposium: Sanitation and groundwater protection.

Tu TA, Tweed S, Dan NP, et al. 2022. Localized recharge processes in the NE Mekong Delta and implications for groundwater quality. Science of The Total Environment, 845(1): 157118. DOI：10.1016/j.scitotenv.2022.157118.

Van Canh D, Duc Nhan D, Kien Chinh N. 2018. Formation and chemistry of the groundwater resource in the Mekong river delta, South Vietnam. Vietnam Journal of Science, Technology and Engineering, 60(1): 57–67. DOI：10.31276/VJSTE.60(1).57.

Wagner F, Tran VB, Renaud FG. 2012. Groundwater Resources in the Mekong Delta: Availability, Utilization and Risks. In F. G. Renaud & C. Kuenzer (Eds.), The Mekong Delta System: Interdisciplinary Analyses of a River Delta (201-220). Springer Netherlands. DOI：10.1007/978-94-007-3962-87.

Wang P, Han Z, Li Y, et al. 2013. The role of groundwater leakage through deep wells for the deformation of groundwater flow: A case study in Cangzhou area. Journal of Groundwater Science and Engineering, 1(2): 80–87. DOI：10.26599/JGSE.2013.9280022.

Wang Z, Wang LJ, Shen JM, et al. 2024. Groundwater recharge via precipitation in the Badain Jaran Desert, China. Journal of Groundwater Science and Engineering, 12(1): 109–118. DOI：10.26599/JGSE.2024.9280009.

Xu Y, Beekman HE. 2019. Review: Groundwater recharge estimation in arid and semi-arid southern Africa. Hydrogeology Journal, 27(3): 929–943. DOI：10.1007/s10040-018-1898-8.

Xu Y, Van Tonder GJ. 2001. Estimation of recharge using a revised CRD method. Water SA, 27(3): 341–343. DOI：10.4314/wsa.v27i3.4977.